Curr Radiol Rep (2014) 2:49
DOI 10.1007/s40134-014-0049-9

Diffusion Imaging of the Head and Neck

Hideomi Yamauchi · Ashok Srinivasan

Published online: 20 March 2014

Abstract Diffusion MR for brain imaging has been well-researched and used clinically for more than a decade, particularly for detection of acute ischemic stroke and evaluation of intracranial cystic lesions. In comparison, its application to the head and neck (H&N) has only attracted interest more recently, as a result of the development of techniques for reducing susceptibility artifacts which are substantially more frequent for the neck than for the brain. In this article we discuss recent advances in diffusion imaging technology and describe clinical applications in the H&N. After reading the article, readers should have a better understanding of the uses and challenges of diffusion imaging of the head and neck.

Keywords Diffusion imaging · Head and neck cancer · Cholesteatoma

Introduction

Diffusion-weighted imaging (DWI) is a molecular MR imaging technique that enables evaluation of water diffusion in a region of interest by using strong, symmetric gradients before and after a 180° refocusing pulse. Unlike application to the brain, application of DWI to the head and neck (H&N) has been fraught with challenges because of abundant fat, geometric distortion, motion, and susceptibility artifacts from air–soft tissue interfaces. In the last few years, however, there has been increasing interest in clinical application of diffusion imaging of the H&N, primarily because of improved technology which has resulted in higher-quality images with fewer artifacts and less image distortion. In this article we discuss the different DWI sequences used in H&N imaging, emphasizing recent technical developments in diffusion imaging. We then discuss current knowledge of clinical applications of DWI for characterization of neck and temporal bone masses, differentiation of nodes, and evaluation of response to tumor treatment.

This article is part of the Topical Collection on *Advanced Imaging of the Head and Neck Region*.

H. Yamauchi · A. Srinivasan (✉)
Department of Radiology, Division of Neuroradiology, University of Michigan Health System, 1500 E Medical Center Drive, B2-A209, Ann Arbor, MI 48109, USA
e-mail: ashoks@med.umich.edu

Techniques

Development of diffusion techniques for adequate imaging of the extracranial H&N in the last decade has depended on strategies used to mitigate artifact and distortion, and improve spatial resolution. The two major techniques used to acquire diffusion images of the head and neck are echo-planar and non-echo-planar, both of which have their advantages and challenges.

Echo-Planar Diffusion Weighted Imaging

Echo-planar (EP) DWI is the technique most widely used for evaluation of the H&N, primarily because the relatively short acquisition time results in insensitivity to bulk motion. Although EP-DWI can be performed as either single or multi-shot sequences, the single-shot echo-planar imaging (SS-EPI) technique has limited spatial resolution and greater geometric distortion, because susceptibility artifacts, especially at air–tissue interfaces. In contrast, multi shot EP-DWI can provide high-resolution images with reduced geometric distortion and a signal-to-noise

ratio (SNR) similar to that of SS-EPI. The major disadvantage of multi shot EP-DWI is its longer acquisition time, which can result in more motion artifacts, for example those resulting from swallowing or breathing [1].

Non-Echo-Planar Diffusion-Weighted Imaging

Different types of non-echo-planar DWI sequence have been used in H&N imaging, including single-shot turbo spin-echo, half-Fourier acquisition single-shot turbo spin-echo (HASTE), periodically rotated overlapping parallel lines with enhanced reconstruction (PROPEL-LER), BLADE, and multi shot turbo spin-echo DWI. Although these modified sequences result in fewer susceptibility artifacts, and enable thinner sections and higher imaging matrices, the disadvantages include longer acquisition time and lower signal-to-noise ratio [2].

Clinical Applications

Improved Characterization of Head and Neck Lesions

Apparent Diffusion Coefficient (ADC)-Based Prediction of Malignancy—Role of Non-Echo-Planar Imaging

There is increasing interest in evaluating the ADC value as an important factor for differentiating between benign and malignant neck soft tissues, both before and after tumor therapy. This is based on the hypothesis of restricted diffusion in tissues with higher cellularity, for example malignancies, with corresponding lower ADC values than normal tissues or benign pathologies with normal or low cellularity, respectively. The challenges in achieving this objective have been susceptibility artifacts, especially at air–soft tissue interfaces, image distortion because of varying neck geometry, and the need to develop appropriate "*b*" values that can be applied clinically and which can be robust and reproducible across institutions. Several studies have reported promising use of non-echo-planar DWI in the H&N region, focusing on its advantages of fewer geometric distortions and susceptibility artifacts than EP-DWI.

In a retrospective study utilizing three sets of b factors (0 and 1,000 s mm^2, 500 and 1,000 s mm^2, and weighted linear regression fit of all *b* values: 0, 100, 300, 500, 700, and 1,000 s mm^2) for ADC measurement using HASTE DWI, the authors showed that pathologic H&N tissues were characterized effectively and high overall accuracy was obtained in prediction of malignancy by all methods. The ADC values of benign tumors were higher than those of malignant tumors, and the highest overall accuracy of 83.3, 86.1, and 88.9 % was obtained when threshold ADC values of 1.24×10^{-3} mm^2 s^{-1} (0–1,000 method), 0.98×10^{-3} mm^2 s^{-1} (500–1,000 method), and 1.23×10^{-3} mm^2 s^{-1} (with weighted linear regression fit) were used for prediction of malignancy [3]. However, in another study comparing detection and delineation of 12 primary tumors and 77 lymph nodes larger than 5 mm by use of pretreatment HASTE and EPI-DWI for head and neck squamous cell carcinoma (HNSCC), Verhappen et al. [4] reported that primary tumors and lymph nodes were more readily visualized by use of EP-DWI than by use of HASTE-DWI, probably because of the lower SNR of the latter sequence. The number of primary tumors and lymph nodes detected by use of pretreatment EP-DWI was higher than that by use of pretreatment HASTE-DWI, with mean numbers of lesions of 88.5 and 69, respectively. Moreover, detection of 91 % of lesions by use of pretreatment EP-DWI was described as good compared with detection of 40 % of the total number lesions by pretreatment HASTE-DWI.

PROPELLER DWI has been proposed as a good technique for reducing susceptibility and motion artifacts. This sequence consists of a multi-shot fast spin-echo pulse that over-samples the center of k-space in concentric rotated rectangular strips and thereby enables correction for in-plane displacement and rotation, image phase as a result of motion, and through-plane motion. Whereas previous studies of PROPELLER DWI of the H&N focused mainly on middle ear cholesteatoma at 1.5T and 3T, and the parotid gland at 1.5T, there has recently been interest in using this technique to differentiate benign and malignant neck soft-tissue lesions. In a prospective study investigating use of PROPELLER DWI to correct distortion and differentiate between benign and malignant H&N solid masses at 3T, the authors found that mean distortion scores for PROPELLER DWI were significantly higher than for EP DWI (3.87 vs. 1.96, and 3.88 vs. 2.00, with *b* values of 1,000 and 500 s mm^2, respectively, $p < 0.001$), indicating that distortion of the mass in PROPELLER DWI was much less than in EPI DWI. In addition, the mean ADC value of 24 malignant solid masses was significantly lower than that of 21 benign solid masses using either PROPELLER DWI or EPDWI, with *b* values of 0 and 1,000 s mm^2 or 0 and 500 s mm^2 ($p < 0.001$). When an ADC value of 1.35×10^{-3} mm^2 s^{-1} was used to predict malignancy in PROPELLER DWI with *b* values of 0 and 1,000 s mm^2, the highest diagnostic accuracy of 88.9 % was obtained, with 95.8 % sensitivity and 81 % specificity. This study showed the technique could be useful for imaging H&N lesions with less distortion; however, the disadvantages include a longer acquisition time and a lower SNR [5].

In our experience of the routine use of EP-DWI for clinical examinations we have obtained better quality images and encountered fewer susceptibility artifacts, even at higher Tesla strength scanning when the appropriate parallel imaging strategies are used. Examples of EP-DWI

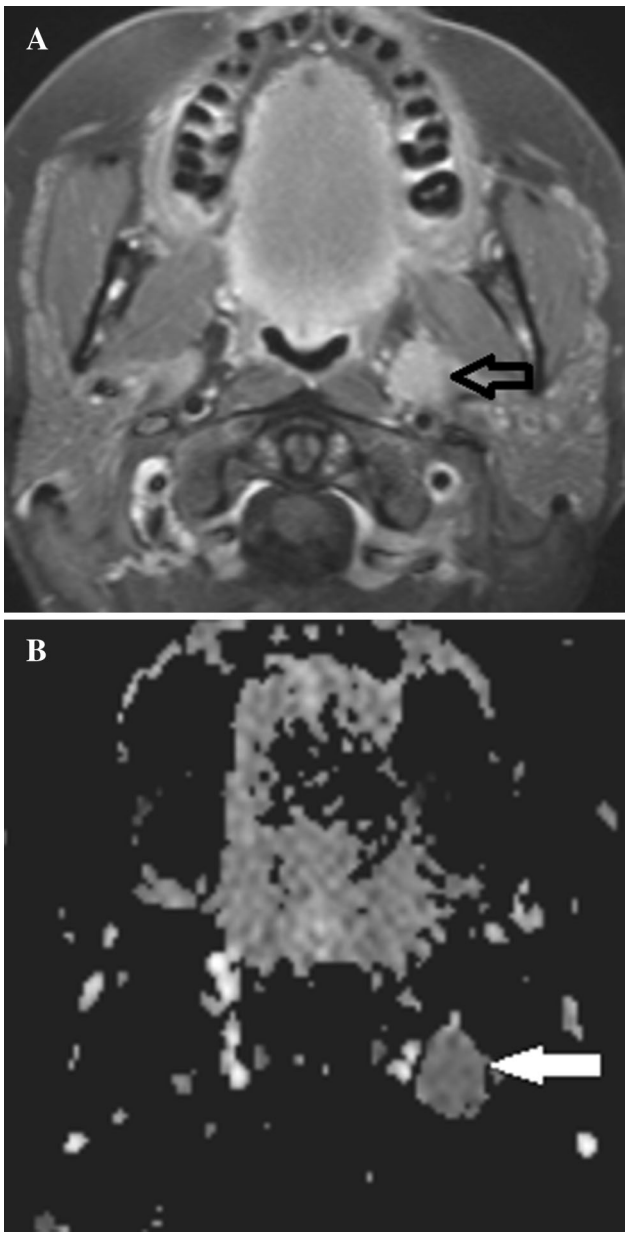

Fig. 1 (**a**) Postgadolinium T1-weighted image of a 45-year-old female shows a well-defined enhancing mass in the left parapharyngeal space (*arrow*). (**b**) The increased signal observed in the corresponding ADC map is indicative of increased ADC values in the mass, which is suggestive of a benign process. This proved to be a benign pleomorphic adenoma

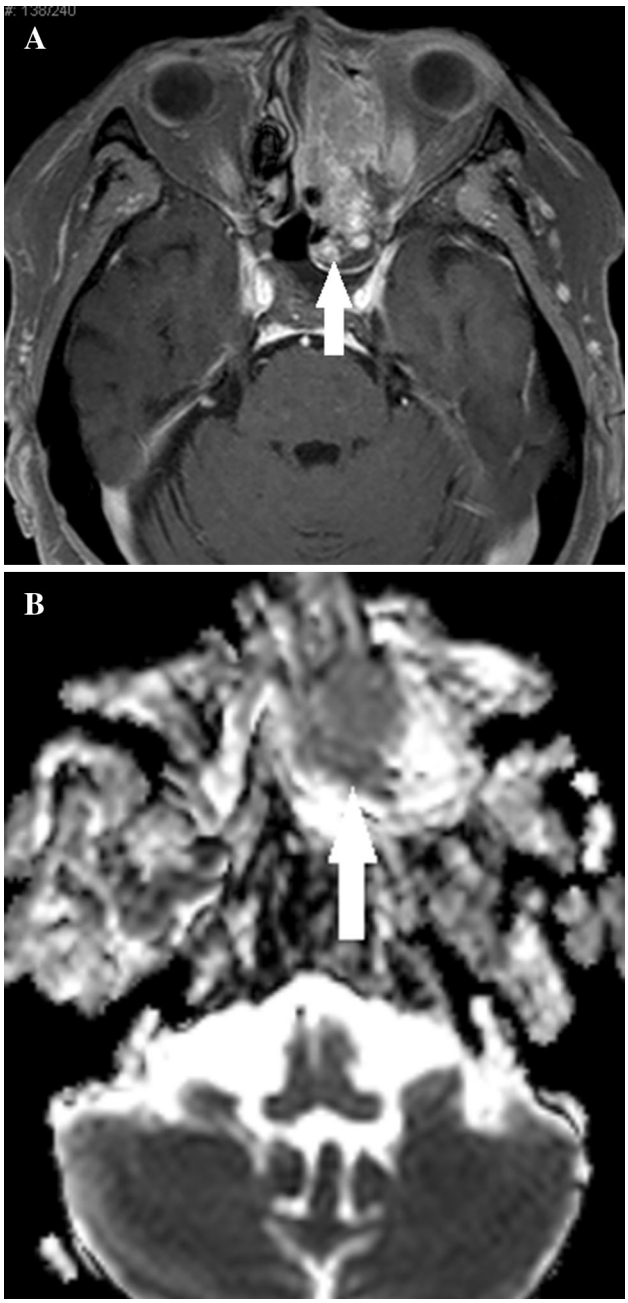

Fig. 2 (**a**) Postgadolinium T1-weighted image of a 52-year-old male shows an ill-defined enhancing mass involving the left nasal cavity (*arrow*). (**b**) The low signal observed in the corresponding ADC map is indicative low ADC values in the mass, suggestive of a highly cellular process, for example a malignancy. This proved to be sinonasal undifferentiated carcinoma (SNUC)

of benign and malignant neck lesions are illustrated in Figs. 1 and 2.

ADC-Based Differentiation of Lymphoma and Carcinoma

In addition to differentiating between benign and malignant lesions, ADC has also been studied as a means of differentiating lymphomas from carcinomas. Ichikawa et al. [6•] reported that ADC-based differentiation of lymphomas from carcinomas was effective for the oropharynx, but not the nasopharynx, when using *b* values of 500 and 1,000 s mm^2. In the oropharynx, overall ADC values for lymphomas ($0.503 \pm 0.099 \times 10^{-3}$ mm^2 s^{-1}) were significantly smaller than those for carcinomas ($0.842 \pm 0.164 \times 10^{-3}$ mm^2 s^{-1}). The ADC threshold of 0.66×10^{-3} mm^2 s^{-1}

discriminated oropharyngeal lymphomas from HNSCC with 100 % sensitivity, 88 % specificity, 93 % accuracy, and 85 % positive and 100 % negative predictive value. In contrast, overall ADC values were similar for nasopharyngeal lymphoma ($0.528 \pm 0.094 \times 10^{-3}$ mm^2 s^{-1}) and nasopharyngeal nonkeratinizing carcinoma ($0.567 \pm 0.057 \times 10^{-3}$ mm^2 s^{-1}), probably because the latter is pathologically distinct from the more common keratinizing squamous cell carcinoma found elsewhere in the H&N. Interestingly, in the oropharynx, well-differentiated HNSCC with heterogeneity on fat-suppressed T2-weighted images had the largest ADC values ($0.957 \pm 0.067 \times 10^{-3}$ mm^2 s^{-1}). The authors also found that poorly differentiated HNSCC could be subdivided into two types on the basis of fat-suppressed T2-weighted images, namely, those with a homogeneous T2 signal and those with a heterogeneous T2 signal, with the more homogeneous lesions having substantially smaller ($<0.8 \times 10^{-3}$ mm^2 s^{-1}) ADC values than the more heterogeneous lesions. Thus, ADC seems a promising tool not only for differentiating carcinomas from lymphomas but also for distinguishing different pathological varieties of oropharyngeal HNSCC.

Lymph Node Characterization by Use of ADC

In previous studies, ADC has been evaluated as a possible biomarker of necrotic areas in metastatic cervical lymph nodes from HNSCC [7, 8]. Recently, in two different studies of necrotic cervical nodes, the authors reported that DWI was helpful in distinguishing tuberculous lymphadenitis from malignancy, and suppurative lymphadenitis from malignancy. Zhang et al. [9] found that the mean ADC value for necrosis was higher in the necrotic portions of metastatic nodes ($2.02 \pm 0.36 \times 10^{-3}$ mm^2 s^{-1}) than in tuberculous nodes ($1.25 \pm 0.15 \times 10^{-3}$ mm^2 s^{-1}) ($p < 0.01$). In addition, the optimum ADC threshold for distinguishing between metastasis and tuberculosis was 1.59×10^{-3} mm^2 s^{-1}, with sensitivity and specificity of 88 and 100 %, respectively. This was also corroborated in another study by Kato et al. [10] in which the ADC of necrotic cervical nodes was shown to be higher in metastatic nodes ($1.46 \pm 0.50 \times 10^{-3}$ mm^2 s^{-1}) than in tuberculous nodes ($089 \pm 0.21 \times 10^{-3}$ mm^2 s^{-1}) ($p < 0.01$). Thus, ADC could prove useful for identification of metastatic nodes in populations in which granulomatous infections such as tuberculosis are also endemic.

Pre-Cancerous Lesions Versus Cancer

In a preliminary study of 33 pathologically proved laryngeal carcinomas and 17 premalignant lesions, the authors were able to use turbo spin-echo DWI (using b values of 1,000 s mm^2) at 3 T to distinguish the two categories with sensitivity, specificity, and accuracy of 100, 88.2, and 96.0 %, respectively; mean ADC values were lower for patients with laryngeal carcinoma ($1.195 \pm 0.32 \times 10^{-3}$ mm^2 s^{-1}) than for those with laryngeal precancerous lesions ($1.780 \pm 0.32 \times 10^{-3}$ mm^2 s^{-1}; $p < 0.001$). On ROC analysis, an ADC cutoff of 1.455×10^{-3} mm^2 s^{-1} was optimum (AUC = 0.956) for distinguishing laryngeal carcinomas and precancerous lesions, and resulted in sensitivity of 94.1 %, specificity of 90.9 %, and accuracy of 92.9 % [11]. Although this is only one preliminary study of its kind, again it confirms the ability of ADC to distinguish tissues with different microstructure.

Correlation with HPV Status

Human papilloma virus (HPV) status is a confirmed prognostic marker in oropharyngeal HNSCC. Patients with HPV-positive HNSCC respond more favorably to chemotherapy and radiation, with better survival than those with HPV-negative HNSCC. Hence, the development of imaging markers to predict this status is of interest to radiologists and surgeons. In a retrospective study of 26 patients with HNSCC confined to the lateral oropharyngeal wall or the base of the tongue, the authors showed that the mean and minimum ADC values for HPV-positive HNSCC were significantly lower than those for HPV-negative HNSCC ($p < 0.01$); the cut-off mean ADC value was 1.027×10^{-3} mm^2 s^{-1}. Sensitivity and specificity of 83.33 and 78.57 %, respectively, were demonstrated for prediction of HPV-positive HNSCC. This thus enabled immediate useful identification of HPV-positive tumors before the results of p16 immunohistochemistry tests were available [12]. More studies are required before DWI can be reliably used to predict HPV status.

Intravoxel Incoherent Motion (IVIM) Imaging

Intravoxel incoherent motion is a term used to describe the effect on DWI signal of intra and extracellular water molecule motion and the motion of microcirculation of blood within small capillaries. Because blood flow in a large vessel within a voxel moves in the same direction, the intravascular protons are in coherent motion. By contrast, in a vessel smaller than a voxel, for example a capillary, the intravascular flow moves in different directions within the same voxel. ADC alone cannot separate pure molecular diffusion from the motion of water molecules in the capillary network. IVIM imaging is a method initially developed by Le Bihan et al. for quantitative assessment of the microscopic translational motion that occurs in each image voxel. Later, Le Bihan et al. and Luciani et al. [13, 14] were able to demonstrate that IVIM imaging can distinguish between pure molecular diffusion and the motion of water molecules in the capillary network in a single voxel

on MRI. i.e. the diffusion and perfusion characteristics, respectively. Recently, several attempts have been made to determine the perfusion and diffusion characteristics by use of IVIM MRI. In a retrospective study assessing perfusion-related (PP) and purely molecular-based (D) diffusion on the basis of an IVIM model (using three *b* values of 0, 500, and 1,000 s mm^2) the authors characterized different types of H&N tumor with distinct IVIM profiles consisting of different proportions of capillary perfusion and pure molecular diffusion components. The *PP* values (lymphomas, 0.09 ± 0.04; SCCs, 0.15 ± 0.04; and malignant salivary gland tumors, 0.22 ± 0.07) and *D* values (0.47 ± 0.07 × 10^{-3} mm^2 s^{-1}, 0.82 ± 0.17 × 10^{-3} mm^2 s^{-1}, and 1.03 ± 0.16 × 10^{-3} mm^2 s^{-1}, respectively) were significantly different among the malignant tumors ($p < 0.01$). These values were also significantly different between pleomorphic adenomas (0.13 ± 0.02 and 1.44 ± 0.39 × 10^{-3} mm^2 s^{-1}) and Warthin tumors (0.19 ± 0.04 and 0.73 ± 0.22 × 10^{-3} mm^2 s^{-1}; $p < 0.01$). *PP* values for malignant salivary gland tumors were significantly different from those for pleomorphic adenomas ($p = 0.01$) and *D* values for malignant salivary gland tumors were significantly different from those for pleomorphic adenomas ($p = 0.002$) and Warthin tumors ($p = 0.007$) [15]. However, substantial overlap of *P* and *D* values was observed for many types of head and neck tumor. In addition, when a multivariable approach using both *PP* and *D* values and time–intensity curve (TIC) profiles was tested, this was able to differentiate between benign and malignant tumors with 97 % accuracy, and enabled diagnosis of different types of tumor with 89 % accuracy. A *PP* less than 0.17 discriminated lymphoma and lymphomatous nodes with Type 4 TIC profiles (enhancement ratio greater than 20 %, with maximum times shorter than 120 s and with washout ratios equal to or greater than 30 % and smaller than 70 %) from Warthin tumors ($PP \geq 0.17$) with the same TIC profile. The same *PP* criterion effectively differentiated between pleomorphic adenomas and schwannomas with Type 2 TIC profiles (enhancement ratio greater than 20 %, and maximum times equal to or longer than 120 s) and high *D* values ($D \geq 1.2$) [16•]. In the future, IVIM may be an additional imaging technique for further characterization of H&N tumors.

Prediction and Monitoring Response to Therapy

Different diffusion characteristics have been studied as potential tools for predicting the outcome of chemoradiation and monitoring early changes in response to chemoradiation. These have included whole-tumor mean ADC, ADC histogram, IVIM results, and fractional change in ADC. Recognition of poor response during the early stages of therapy can help identify patients for alternative therapy, for example escalated doses of radiation, and thereby affect patient outcomes.

Pre-treatment Assessment

Srinivasan et al. [17] generated whole-tumor mean ADC values, by drawing freehand regions of interest along the margins of the entire primary tumor on all axial slices, and also created ADC histograms. They found whole-tumor mean ADC were significantly different ($p = 0.03$) for patients with positive and negative outcomes (1.18 vs. 1.43, respectively). ADC histogram analysis was also helpful for tumors with more than 45 % of their volume below the ADC threshold of 1.15 × 10^{-3} mm^2 s^{-1}, for which a positive outcome was more likely (accuracy, 77 %). In another study, Ahn et al. [18] reported that the mean ADC at $b = 2{,}000$ s mm^2 was significantly higher ($p < 0.05$) for well-differentiated HNSCC (881 ± 131 × 10^{-6} mm^2 s^{-1}) than for moderately differentiated and poorly differentiated HNSCC (770 ± 163 and 780 ± 158 × 10^{-6} mm^2 s^{-1}, respectively); they also showed that the kurtosis ratio ($Kurtosis_{ADC2000}$/$Kurtosis_{ADC1000}$) was significantly higher for poorly differentiated HNSCC (115 ± 10 %) than for well differentiated and moderately differentiated HNSCC (91 ± 21 % and 86 ± 26 %, respectively).

By using the IVIM model, Hauser et al. [19] studied the perfusion-related variable *f*, the baseline diffusion-related coefficient *D*, and ADC (using eight different *b* values: 0, 50, 100, 150, 200, 250, 700, 800). High initial *f* (13.1 ± 4.1 % vs. 9.1 ± 2.4 %) before therapy and ADC (1.17 ± 0.08 × 10^{-3} mm^2 s^{-1} vs. 0.98 ± 0.19 × 10^{-3} mm^2 s^{-1}) were associated with poor short-term outcome (locoregional failure, distant metastases, or death) after 7.5 months follow up. At first follow up (six weeks after conclusion of the therapy), *D*, *f*, and ADC were shown to increase for all primary responders. In yet another study, the authors reported that pretreatment mean ADC can be used as a predictive biomarker for induction chemotherapy response in NPC [20]. Overall, these studies demonstrate that pre-treatment DWI could become an important predictor of the success of therapy before commencement of treatment.

Early Treatment Monitoring

Although anatomical images may not enable sensitive assessment of early response to chemoradiation, it might be possible to overcome this problem by using DWI to evaluate the changes in water diffusion that occur as a result of breakdown of tissue microstructure in response to treatment. In a study evaluating the fractional change in ADC (ΔADC) as an imaging biomarker for predicting response three weeks after the start of treatment, the $\Delta ADC_{primary}$ after three weeks of treatment was significantly lower for lesions with locoregional failure (LRF) than for those with locoregional control

(LRC). In multivariate analysis, only $\Delta ADC_{primary}$ was significantly associated with LRC. In addition, the $\Delta ADC_{primary}$ threshold value of 0.24 resulted in 100 % sensitivity and 100 % negative predictive value for the prediction of LRC. Furthermore, during comparison of progression-free survival by using the $\Delta ADC_{primary}$ threshold value of 0.24 to distinguish the LRC group from the LRF group, patients with $\Delta ADC_{primary} \geq 0.24$ had better prognosis than those with $\Delta ADC_{primary} < 0.24$ [21••]. Thus, a high negative predictive value of $\Delta ADC_{primary}$ may aid identification of patients with LRF to chemoradiotherapy at an early phase of treatment, thereby aiding individualization of therapy.

These observations have been corroborated in other studies also. Vandecaveye et al. [22] reported that ADC change three weeks post-treatment can predict treatment response with greater accuracy than morphological imaging assessment. Hong et al. [23] showed that the rate of change of ADC two weeks after the start of radiotherapy was significantly different between groups with and without residual tumor, and was an independent prognostic factor three - months after the end of radiotherapy for nasopharyngeal carcinoma (NPC). Thus, assessment of ADC should be considered when determining early treatment response.

Post Treatment Assessment

Assessment of the tumor after completion of therapy is crucial to identifying residual tumor and determining follow-up options. However, differentiation of recurrent tumor from post-treatment changes by use of conventional anatomical images alone can often be challenging. DWI can be helpful in this assessment, as shown by some recent studies.

Several studies have reported that ADC was lower recurrent tumors than for post-therapy change, presumably because of the increased cellularity of recurrent tumors [24, 25]. In a retrospective study using a high b value ($b = 2{,}000$ s mm^2), Hwang et al. [26•] found that the mean ADC_{ratio} ($ADC_{2000}/ADC_{1000} \times 100$) was higher for recurrent tumors than for post-treatment changes, presumably because of a larger slow diffusion component. Examples of post-operative granulation tissue and recurrent malignancy are illustrated in Figs. 3 and 4, respectively.

Evaluation of Cholesteatoma

Although second-look surgery is often required to exclude residual or recurrent cholesteatoma, disadvantages include a greater risk of complications, unnecessary surgery, and the need to repeat general anesthesia. Both EP and non-EP DWI have been used as imaging options for primary and residual or recurrent cholesteatoma; the non-EP techniques of HASTE, BLADE, PROPELLER and turbo field-echo with diffusion-sensitized driven-equilibrium (TFE-DSDE) are less sensitive to magnetic susceptibility artifacts and result in less anatomical distortion than images produced with EP-DWI.

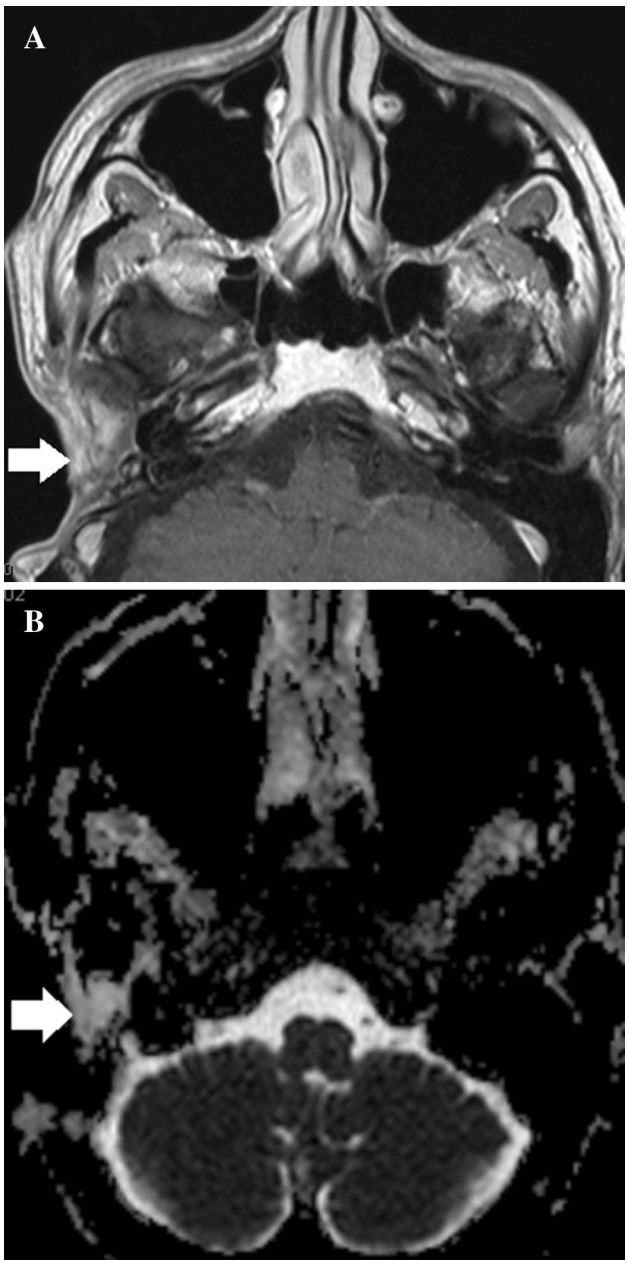

Fig. 3 (**a**) Postgadolinium T1-weighted image from a 65-year-old male with previous surgery for squamous cell carcinoma of the pinna shows an enhancing lesion posterior to the right temporomandibular joint (*arrow*). (**b**) The corresponding ADC map shows high signal (*arrow*) indicating increased ADC values, and suggestive of a benign process. This was biopsied and revealed to be benign granulation tissue

In a meta-analysis evaluating the accuracy of non-EP-DWI for identification of cholesteatoma, Li et al. [27] showed that overall combined sensitivity of non-EP-DWI in detection of cholesteatoma was 0.94 (confidence

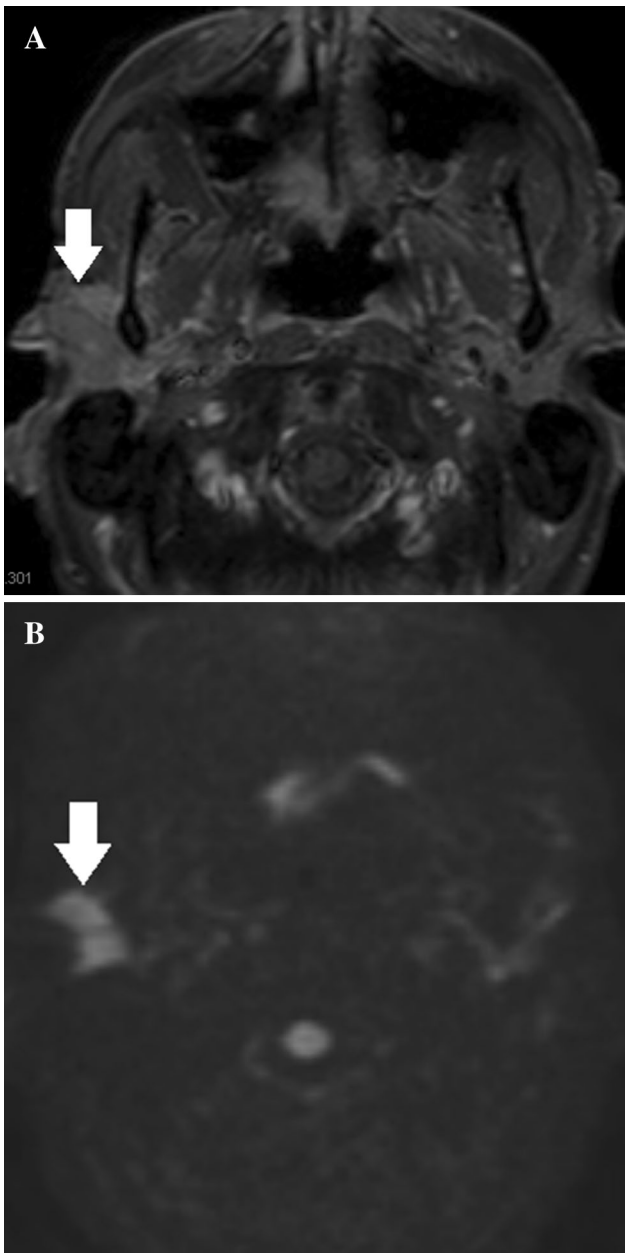

Fig. 4 (**a**) Postgadolinium T1-weighted image **a** from a 38-year-old male with previous parotid adenosquamous carcinoma shows an enhancing lesion involving the parotid bed (*arrow*). (**b**) DWI with $b = 1{,}000$ shows increased diffusion signal (*arrow*) and corresponding low ADC (*not shown*), which is suggestive of malignancy. This was a biopsy-proved recurrent parotid carcinoma

interval, 0.80–0.98) and specificity was 0.94 (confidence interval, 0.85–0.98). Most false-negative results were because of cholesteatoma pearls measuring <3 mm in size. In a prospectively study of TFE-DSDE for diagnosis of middle-ear cholesteatoma, Yamashita et al. [28] reported significantly higher sensitivity (83.3 %) and accuracy (90.0 %) of this technique compared with SS-EP DWI (sensitivity = 35.0 % and accuracy = 66.7 %). By using TFE acquisition instead of EP acquisition, susceptibility artifacts were greatly reduced. In another prospective blinded study comparing non-EP and EP-DWI for detection of residual/recurrent cholesteatoma in long-term follow-up after one-step canal-wall-down obliteration surgery, the authors showed that six of the seven non-EP positive cases (two patients clinically without cholesteatoma) underwent surgical revision with confirmation of cholesteatoma; however, the EP technique detected cholesteatoma in only two of the six surgically confirmed cholesteatomas. In addition, the inter-rater agreement (0.91) between the reviewers was significantly higher with the non-EP technique [29]. Although these studies show DWI is important for assessment of residual/recurrent cholesteatoma, it is also important to know if the site and extent predicted by DWI correlate with the final surgical results. In a study evaluating this correlation, the authors showed that non-EP DWI detected the precise location and extent of cholesteatoma in 49 of 50 cases (98 %). The correlation of preoperative radiologic images with intraoperative clinical findings was also good with regard to tympanic and mastoid cholesteatoma [30•]. Our experience has also shown that DWI is an excellent technique for detection of recurrent cholesteatoma.

Combination of DWI and FDG PET/CT

FDG PET/CT is an established functional imaging tool for evaluation of HNSCC. Recent studies have suggested that the combination of FDG PET/CT and DWI can be beneficial with good correlations of standardized uptake value (SUV) and ADC values reported for both primary tumors and metastatic lymph nodes.

In a retrospective study of DWI and FDG PET/CT for evaluation of 24 primary HNSCC, Nakajo et al. [31] showed a negative correlation between SUV_{max} and ADC (0.566, $p = 0.005$) with optimum cutoff values of 12.1 for SUV_{max} and 0.88 for ADC. By contrast, in a retrospective study of 34 primary HNSCC. Varoquaux et al. [32] reported there was no statistically significant association between ADC and SUV values; they were independent biomarkers of HNSCC. Later, in a prospective study of metastatic neck lymph nodes of HNSCC, a different set of authors were able to show there were statistically significant inverse correlations between ADC and SUV for metastatic lymph nodes [33]. In yet another prospective study evaluating the diagnostic accuracy of software-based fusion of ^{18}F-FDG-PET-MRI plus DWI for detection of cervical lymph node metastases in HNSCC, the authors showed that the sensitivity, specificity, positive predictive value, negative predictive value, and accuracy were, respectively, 53, 97, 67, 95, and 92 % for ^{18}F-FDG-PET-MRI plus DWI; 63, 99, 86, 96, and 95 % for US; and 30,

97, 56, 92, and 90 % for ^{18}F-FDG-PET/CT. However, diagnostic accuracy of node detection for patients with oral malignancies was not significantly different for ^{18}F-FDG-PET-MRI plus DWI and US or for ^{18}F-FDG-PET-MRI plus DWI and ^{18}F-FDG-PET/CT [34]. These studies indicate further research is needed to evaluate the utility of true simultaneous acquisition of multi-mode PET and MRI.

Thyroid Evaluation with DWI

Evaluation of thyroid nodules is typically performed with ultrasound; however, there studies have evaluated the potential role of DWI in this field.

Shi et al. [35] reported the utility of DWI (*b* values 150, 300, and 500 s mm^2) for differentiating malignant from benign thyroid nodules and the pathologic correlation with ADC values for thyroid nodules ($p < 0.01$). They showed that DWI signal intensity was higher for most (69 %) benign thyroid nodules than for most (65 %) malignant thyroid nodules, possibly because of the relative abundance of colloid follicles, and microcysts in such benign thyroid nodules as adenoma and nodular goiter. Moreover, they found that the ADC value was significantly lower for malignant nodules and thyroiditis than for adenoma and nodular goiter. Their pathological correlation demonstrated that increased cell density with relatively marked desmoplastic response resulted in a decrease in ADC for thyroid carcinoma, whereas abundant follicles and extracellular fluid with less cell density resulted in higher ADC values for adenoma and nodular goiter. The abundant lymphocytes, fibrous tissue, and atrophic follicles possibly explained the lower ADC value for thyroiditis.

Correlation with Pathological Grades

The ability of imaging to predict pathological grades of tumors has always been of interest for all body parts, because of its prognostic implications. In a study evaluating two different *b* values (the standard 1000 s mm^2 and a high 2,000 s mm^2) for differentiating the histologic grade in patients with HNSCC, Yun et al. [36] showed that the ADC values for well differentiated HNSCC were significantly different from those for poorly differentiated HNSCC ($p < 0.001$) for both *b* values. However, significant a difference between the ADC values for moderately differentiated and poorly differentiated HNSCC was noted only for $b = 2000$ s mm^2 ($p = 0.014$). They hypothesized that the loss of keratinization and intercellular bridges for poor histologic grades made the tissue more compact, resulting in lower ADC values. They also showed that the ADC decreases for the HNSCC, paravertebral neck muscles, and CSF were 22.4, 45.8, and 48.4 %, respectively, when the *b* value was increased from 1,000 to 2,000 s mm^2. In conclusion, they suggested that the magnitude of the ADC decrease after changing the *b* value may aid differentiation between tumor and normal structures.

Conclusion

In summary, imaging has made rapid advances in the past few decades, especially in its ability to generate higher-resolution images in a time-efficient manner and to enable evaluation of structures of the order of a few millimeters. Review of the recent literature shows the potential of advanced imaging modalities, for example diffusion and perfusion imaging, to aid better characterization and evaluation of tissues. In particular, addition of diffusion imaging to high-resolution anatomical imaging of the H&N has the potential to enable more comprehensive evaluation of tissues by providing both structural and functional information. This can enable better tissue characterization and aid management decisions, with the eventual objective of improving patient outcomes.

Compliance with Ethics Guidelines

Conflict of Interest H Yamauchi and A Srinivasan declares no conflicts of interest.

Human and Animal Rights and Informed Consent All studies by the authors involving animal and/or human subjects were performed after approval by the appropriate institutional review boards. When required, written informed consent was obtained from all participants.

References

Papers of particular interest, published recently, have been highlighted as:
- • Of importance
- •• Of major importance

1. Yamashita K, Yoshiura T, Hiwatashi A, et al. Detection of middle ear cholesteatoma by diffusion-weighted MR imaging: multishot echo-planar imaging compared with single-shot echo-planar imaging. AJNR Am J Neuroradiol. 2011;32:1915–8.
2. Mas-Estelles F, MateosFernandez M, Carrascosa-Bisquert B, et al. Contemporary non–echo-planar diffusion-weighted imaging of middle ear cholesteatomas. Radiographics. 2012;32:1197–213.
3. Sakamoto J, Sasaki Y, Otonari-yamamoto M, et al. Comparison of various methods for quantification of apparent diffusion coefficient of head and neck lesions with HASTE diffusion-weighted MR imaging. Oral Surg Oral Med Oral Pathol Oral Radiol. 2012;114:266–76.
4. Verhappen M, Pouwels P, Ljumanovic R, et al. Diffusion-weighted MR imaging in head and neck cancer: comparison between half-fourier acquired single shot turbo spin-echo and EPI techniques. AJNR Am J Neuroradiol. 2012;33:1239–46.
5. Chen X, Xian J, Wang X, et al. Role of periodically rotated overlapping parallel lines with enhanced reconstruction diffusion-

weighted imaging in correcting distortion and evaluating head and neck masses using 3 T MRI. Clin Radiol. 2013;69(4):403–9.
6. • Ichikawa Y, Sumi M, Sasaki M, et al. Efficacy of diffusion-weighted imaging for the differentiation between lymphomas and carcinomas of the nasopharynx and oropharynx: correlations of apparent diffusion coefficients and histologic features. AJNR Am J Neuroradiol. 2012;33:761–766. *Showed a promising value of ADC threshold discriminated oropharyngeal lymphomas from SCCs.*
7. Abdel Razek AA, Soliman NY, Elkhamary S, et al. Role of diffusion-weighted MR imaging in cervical lymphadenopathy. Eur Radiol. 2006;16:1468–77.
8. Holzapfel K, Duetsch S, Fauser C, et al. Value of diffusion-weighted MR imaging in the differentiation between benign and malignant cervical lymph nodes. Eur J Radiol. 2009;72:381–7.
9. Zhang Y, Chen J, Shen J, et al. Apparent diffusion coefficient values of necrotic and solid portion of lymph nodes: differential diagnostic value in cervical lymphadenopathy. Clin Radiol. 2013;68:224–31.
10. Kato H, Kanematsu M, Kato Z, et al. Necrotic cervical nodes: usefulness of diffusion-weighted MR imaging in the differentiation of suppurative lymphadenitis from malignancy. Eur J Radiol. 2013;82:e28–35.
11. Shang D-S, Ruan L-X, Zhou S-H, et al. Differentiating laryngeal carcinomas from precursor lesion by diffusion-weighted magnetic resonance imaging at 3.0 T: a preliminary study. PLoS One. 2013;8:e68622.
12. Nakahara M, Saito N, Yamaguchi H, et al. Use of quantitative diffusion-weighted magnetic resonance imaging to predict human papilloma virus status in patients with oropharyngeal squamous cell carcinoma. Eur Arch Otorhinolaryngol. 2013.
13. Le Bihan D, Breton E, Lallemand D, et al. Separation of diffusion and perfusion in intravoxel incoherent motion MR imaging. Radiology. 1988;168:497–505.
14. Luciani A, Vignaud A, Cavet M, et al. Liver cirrhosis: intravoxel incoherent motion MR imaging—pilot study. Radiology. 2008;249:891–9.
15. Sumi M, Nakamura T. Head and neck tumors: assessment of perfusion-related parameters and diffusion cofficients based on the intravoxel incoherent motion model. AJNR Am J Neuroradiol. 2013;34:410–41.
16. • Sumi M, Nakamura T. Head and neck tumors: combined MRI assessment based on IVIM and TIC analysis for the differentiation of tumors of different histological types. Euro Radiol. 2014;24:223–231. *This study of combined use of IVIM parameters and TIC files showed high accuracy to differentiate between benign and malignant and between different histological types in head and neck tumors.*
17. Srinivasan A, Chenevert T, Dwamena B, et al. Utility of pretreatment mean apparent diffusion coefficient and apparent diffusion coefficient histograms in prediction of outcome to chemoradiation in head and neck squamous cell carcinoma. J Comput Assist Tomogr. 2012;36:131–7.
18. Ahn S, Choi S, Kim Y, et al. Histogram analysis of apparent diffusion coefficient map of standard and high b-value diffusion MR imaging in head and neck squamous cell carcinoma. Acad Radiol. 2012;19:1233–40.
19. Hauser T, Essig M, Jensen A, et al. Characterization and therapy monitoring of head and neck carcinomas using diffusion-imaging-based intravoxel incoherent motion parameters-preliminary results. Neuroradiology. 2013;55:527–36.
20. Zheng D, Chen Y, Chen Y, et al. Early assessment of induction chemotherapy response of nasopharyngeal carcinoma by pretreatment diffusion-weighted magnetic resonance imaging. J Comput Assist Tomogr. 2013;37:673–80.
21. •• Matoba M, Tuji H, Toyoda I, et al. Fractional change in apparent diffusion coefficient as an imaging biomarker for predicting treatment response in head and neck cancer treated with chemoradiotherapy. AJNR Am J Neuroradiol. 2013. *Demonstrated the high negative predictive value of fractional change in ADC to predict treatment response to chemoradiotherapy at an early phase of treatment.*
22. Vandecaveye V, Dirix P, Keyzer F, et al. Diffusion-weighted magnetic resonance imaging early after chemoradiotherapy to monitor treatment response in head-and-neck squamous cell carcinoma. Int J Radiat Oncol Biol Phys. 2012;82:1098–107.
23. Hong J, Yao Y, Zhang Y, et al. Value of magnetic resonance diffusion-weighted imaging for the prediction of radiosensitivity in nasopharyngeal carcinoma. Otolaryngol Head Neck Surg. 2013;149:707–13.
24. Vandecaveye V, De Keyzer F, Nuyts S, et al. Detection of head and neck squamous cell carcinoma with diffusion weighted MRI after (chemo) radiotherapy: correlation between radiologic and histopathologic findings. Int J Radiat Oncol Biol Phys. 2007;67:960–71.
25. Abdel Razek AA, Kandeel AY, Soliman N, et al. Role of diffusion-weighted echo-planar MR imaging in differentiation of residual or recurrent head and neck tumors and post-treatment changes. AJNR Am J Neuroradiol. 2007;28:1146–52.
26. • Hwang I, Choi S, Kim Y, et al. Differentiation of recurrent tumor and posttreatment changes in head and neck squamous cell carcinoma: application of high b-value diffusion-weighted imaging. AJNR Am J Neuroradiol. 2013;34:2343–2348. *Demonstrated a promising value of ADC_{ratio} calculated from ADC_{1000} and ADC_{2000}.*
27. Li P, Linos E, Gurgel R, et al. Evaluating the utility of non-echo-planar diffusion-weighted imaging in the preoperative evaluation of cholesteatoma: a meta-analysis. Laryngoscope. 2013;123:1247–50.
28. Yamashita K, Yoshiura T, Hiwatashi A, et al. High-resolution three-dimensional diffusion-weighted imaging of middle ear cholesteatoma at 3.0 T MRI: usefulness of 3D turbo field-echo with diffusion-sensitized driven-equilibrium preparation (TFE-DSDE) compared to single-shot echo-planar imaging. Eur J Radiol. 2013;82:e471–5.
29. Edefeldt L, Stromback K, Danckwardt-lilliesrom N, Raskandersen H, et al. Non-echo planar diffusion-weighted MRI increases follow-up accuracy after one-step canal wall-down obliteration surgery for cholesteatoma. Acta Otolaryngol. 2013;133:574–83.
30. • Migirov L, Wolf M, Greenberg G, et al. Non-EPI DW MRI in planning the surgical approach to primary and recurrent cholesteatoma. Otology Neurotology. 2013;35:121–125. *Showed if the site and extent of cholesteatoma predicted by DWI correlate with the final surgical results.*
31. Nakajo M, Nakajo M, Kajiya Y, et al. FDG PET/CT and diffusion-weighted imaging of head and neck squamous cell carcinoma: comparison of prognostic significance between primary tumor standardized uptake value and apparent diffusion coefficient. Clin Nucl Med. 2012;37:475–80.
32. Varoquaux A, Rager O, Lovblad K-O, et al. Functional imaging of head and neck squamous cell carcinoma with diffusion-weighted MRI and PET/CT: quantitative analysis of ADC and SUV. Eur J Nucl. 2013;40:842–52.
33. Nakamatsu S, Matsusue E, Miyoshi H, et al. Correlation of apparent diffusion coefficients measured by diffusion-weighted MR imaging and standardized uptake values from FDG PET/CT in metastatic neck lymph nodes of head and neck squamous cell carcinomas. Clin Imaging. 2012;36:90–7.
34. Heusch P, Sproll C, Buchbender C, et al. Diagnostic accuracy of ultrasound, ^{18}F-FDG-PET/CT, and fused ^{18}F-FDG-PET-MR

images with DWI for the detection of cervical lymph node metastases of HNSCC. Clin Oral Invest. 2013.
35. Shi H, Feng Q, Qiang J, et al. Utility of diffusion-weighted imaging in differentiating malignant from benign thyroid nodules with magnetic resonance imaging and pathologic correlation. J Comput Assist Tomogr. 2013;37:505–10.
36. Yun T, Kim J, Kim K, et al. Head and neck squamous cell carcinoma: differentiation of histologic grade with standard- and high-b-value diffusion-weighted MRI. Head Neck. 2013;35: 626–31.